Experimental investigation of forced flow regime transition in a dual bell nozzle by secondary fluidic injection

Luc Léger, Vladeta Zmijanovic, Mohammed Sellam, Amer Chpoun

Version of Record: https://www.sciencedirect.com/science/article/pii/S0142727X21000485
Manuscript_71a7e2a6f59234a006da3230ee64489b

Experimental investigation of forced flow regime transition in a dual bell nozzle by secondary fluidic injection

L. Léger[(1)], V. Zmijanovic[(1)], M. Sellam[(2)], A. Chpoun[(2)]

(1) ICARE, CNRS ; Orléans, France

(2) LMEE ; Univ. Evry, Université Paris-Saclay, Evry, France

Corresponding author: M. Sellam, mohamed.sellam@univ-evry.fr

Key words: dual bell nozzle, flow control, supersonic flow, transition regime, nozzle flow

Abstract:

Experiments on an axisymmetric dual-bell nozzle were performed at EDITH nozzle test facility of CNRS in Orléans, France. The main purpose of the study was to explore the possibility of controlling the flow regime transition by a secondary fluidic injection in the dual bell nozzle. The main focus of the present paper is to investigate the impact of the secondary injection parameters on the flow regimes transition in such nozzles. Secondary injection has been found to effectively control the flow regime transition and consequently to increase the propulsive performance of the device. It has also been pointed out that even a very low injected secondary mass flow rate leads to the control of the transition and contributes to reducing the lateral loads which can exist, moreover, when transitions are operated without injection.

Introduction:

During the last two decades, a renewed interest in space propulsion can be observed. This surge in activity can be attributed to the emergence of new nations as well as private competitors in the civilian launch market. The main objective is to maximize the payloads and/or to reduce the amount of propellants for a given mission. Supersonic nozzles are crucial in propulsion systems based on gas acceleration in rocket engines. Thereby they offer a certain margin of progress in this regard, by optimizing the flow for the different ambient conditions of the flight. The Dual Bell Nozzle (DBN), as an altitude adaptive concept for rocket jet engines, can be an interesting alternative to the classical single-profile nozzles in use nowadays [1[2, [3]. Basically, the DBN operates without any moving mechanical parts, which would increase the engine weight and provide additional complexities, nor any additional film-cooling device. Hence, it provides a high reliability and simple straightforward optimization. A recent study carried out at the German DLR institute evaluated the performance gain of the DBN compared to a conventional nozzle, for the current European launcher Ariane 5, up to 490 kg of payload increase for a geostationary orbit mission [4].

The proposed study is part of the development of innovative nozzles used in rocket engines. Basically, a dual bell nozzle profile is designed by two different contours joining at a junction point where a slope break is imposed. The first part, designed according to an ideal truncated contour (TIC) or a thrust optimized contour (TOC), generates a flow adapted for operation at low altitudes (in this phase the second part of the nozzle is inoperative). The second part, designed to produce a zero, negative or positive wall pressure gradients, is suitable for high altitude operation. The resulting DBN nozzle operates in these two altitude ranges. Swan first proposed the concept of step-nozzle] in his thesis work at CalTech JPL in the mid-1940s [5]. The aim of the investigation was to explore the possibilities of increasing the performance of rocket vehicles by using multi-step conical nozzles. One of the conclusions of the study was that more than 2 steps nozzle do not significantly change the performance. Improvement of this performance was confirmed at JPL study reported by Foster and Cowles [6]. The dual bell nozzle, as an altitude adaptive nozzle concept, was first patented by Rocketdyne in the 1960s [7]. The control of the transition between the two modes of operation of the nozzle remains, up today, a subject of investigation both theoretically and experimentally. Experimental studies show that the transition between these two regimes takes place before of the theoretical optimal transition point, is non-axisymmetric and results in loss of specific impulse (Figure 1). It also generates undesired side loads [8, [9]. The idea of bringing the transition toward the optimal point, by injecting a secondary fluid, is the main purpose of this study. The objective is therefore to control (to delay) the change of regime to reduce the specific impulse loss and to reduce side loads.

Over the past two decades, the dual bell flow field characteristics and the separation transition mechanism have been extensively investigated. The thermodynamic properties of the fluid and the geometric parameters of the nozzle and their influence on the transition from sea level to altitude modes have been discussed by Genin et al. [8[11], Verma et al [12[15] and Reijasse et al. [16]. The influence of nozzle geometry and flow features on the transition has also been numerically investigated by Martelli et al. [17] and Nasuti et al. [18]. These studies showed, as reported in DLR investigations, that the geometric features, particularly the inflection angle and the relative length of the extension part, can affect the behavior and speed of transition. Nurnberger-Genin and Stark [10] proposed a transition prediction model and studied the separation transition mechanism by focusing on the oblique shock wave motion from the inflexion point to the extension section. The extension wall profile choice is also an important aspect of the problematic to achieve the desired transition and performance criteria: The favorable wall pressure gradient (Negative wall Pressure Gradient NPG) extension would theoretically deliver the higher thrust rate, however this design is prone to different flow separation instabilities ([1], [2], [9]), analogues to that of the single profile conventional nozzles [14]. The constant wall pressure extension (CP) profile is generally better considered and adopted by researchers and engineers as the reference extension nozzle design due to its more stable separated flow feature. However, it also features the sneak transition. On the other hand, some studies as in Nasuti et al. [18] reported shorter transition times in the cases of positive wall pressure gradient (PPG) extension design. Contrary to the NPG extension design, adverse pressure gradient (APG) contour decrease the sneak transition phenomena but produces slightly lower thrust performance and could generate higher side loads ([18], [19]). The regime transition in DBN is also affected by the jet oscillations and buffeting phenomena. As studied by Verma et al.[15] Martelli et al. [17], Proshchanka et al.[20], external or internal sources of acoustic noise can be transmitted, through the separated subsonic flow region, toward the internal flows and can thus affect the transition. Recently a detailed study was conducted at the German DLR to assess

the impact of sea-level transitioning dual bell on the payload mass for a multitude of nozzle contours [21]. The transition regime is taking place during the transient engine start-up at sea-level, such that the side loads are supported on the ground by the launch pad. This design may provide undeniable advantages concerning the side loads, which prevent the use of dual-bell nozzles, however the gain in performance, notably in terms of specific impulse for the two flow regimes, is yet to be achieved.

Transition control by a tangential fluidic injection is a concept that is already used in propulsion systems, equipped with a turbo pump exhaust gas, for the purpose of cooling the second part of the nozzle. The film cooling has been studied previously [22], [23], [24] and potential benefit has been discussed. However, tangential injection adds complexity to the system and don't allow to solve the lateral loads apparition. In this experimental study, we propose to explore the possibility of controlling flow regime transition, inside a DBN nozzle, by radial fluid injection downstream of the contour inflection point.

Transversal secondary injection at the inflection location into the base nozzle in goal to control the separation and transition in DBN was investigated and reported by Tomita et al. [25]. They have reported that use of secondary injection method of active control has a limited effect on the value of the transition NPR and also diminished the base nozzle thrust coefficient during the secondary injection operation. It was also reported that at least 4% of the injected mass flow rate is required to detect any positive effect of secondary injection on the separation sequence. With the same secondary injection setup, Ferrero et al. [26] numerically showed that the transition is effectively delayed by injecting 7.7 % of nozzle mass flow rate.

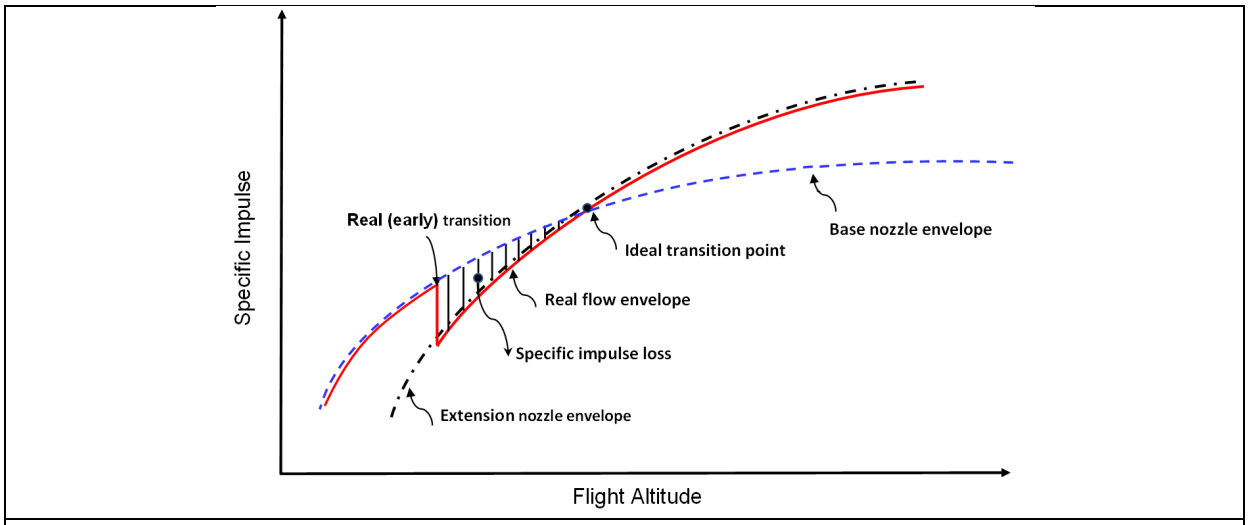

Figure 1 : Performance characteristics of a dual bell nozzle compared with two baseline bell-type nozzles as a function of flight altitude. (derived from [3]).

Nonetheless, as reported by investigations on thrust vector control by secondary fluidic injection [27], [28], [29], this method needs to be carefully optimized in a rocket nozzle in order to be used effectively. Indeed, the secondary injection in a supersonic cross-flow acts as an obstacle which leads to a bow shock and a wall separation of the oncoming flow, and consequently to an adverse wall-pressure gradient in the neighbor zone upstream of the injection port. It was shown [27] that the position of the secondary injection, the mass flow ratio, the heat capacities as well as the secondary to primary molar mass ratio have a strong influence on the effectiveness of the concept.

Inspired from these investigations, the approach presented in the present work suggests setting the secondary injection downstream of the inflection point unlike the previous works. By this way, the main flow must undergo same shock-separation interaction mechanisms described above when meeting the fluidic obstacle. The adverse pressure gradient occurring upstream the injection orifice, coupled with the adverse pressure gradient (APG), dominating the downstream inflection region, must prevent the non-matured nozzle flow to early transit to the extension section, and then to delay the transition NPR towards the optimal point. This active method of transition control, first proposed and patented in [30, [31], is found to be innovative, very simple to implement and inexpensive.

In a precedent and recent study on controlled flow regime transition in a dual bell nozzle by secondary radial injection [32], we have investigated the effect of a constant mass flow rate secondary injection on the properties of flow regime transition. We have showed that the transition and retransition NPR are strongly impacted by a secondary radial injection placed in the extension nozzle. The transition and retransition NPR is increased, allowing a significant increase of the thrust. The side loads during the transition, when the secondary injection is applied, have been found to be significantly reduced for a secondary to primary mass flow rates ratio of 2.2%. In this study the regime transition was obtained by varying the ambient pressure. In the present study, the main nozzle NPR was kept constant and where the flow regime transition and retransition were obtained by varying the secondary injection masse flow rate.

1) Experimental setup and dual-bell nozzle design parameters

Experiments on axisymmetric dual-bell nozzle were performed in the EDITH nozzle test facility of CNRS in Orléans, France. EDITH, initially a blow-down type wind tunnel depicted in Figure 2, was arranged and set, by the authors of this study as a nozzle test facility. The wind-tunnel test chamber provides a low ambient pressure environment by means of two powerful vacuum pumps of 345 kW of combined power. The tested nozzle is mounted on a force-balance frame in the depressurized test section. Dry air from the storage tanks of a total 320 l at a pressure of 300 bars is regulated to 3.5 bars total pressure before being discharged through the dual-bell nozzle into the depressurized test section. The air is supplied via 8 mm pipeline system to the pressure regulator and after to a radial flow-splitter. Through the six 8 mm tubes and their evenly distributed injectors, air is supplied to the settling chamber of 160 mm diameter and 200 mm length before being exhausted through the nozzle into the depressurized test section of the tunnel. Pressures are measured by mean of Baumer TED6 transducers: in the range of 0 to 100 ± 0.1 kPa for the test section, while 100 to 600 ± 1 kPa range is used for pressure measurements in the settling chamber. The experimental setup also provides visual access to the nozzle exhaust jet for Schlieren visualization and camera recording.

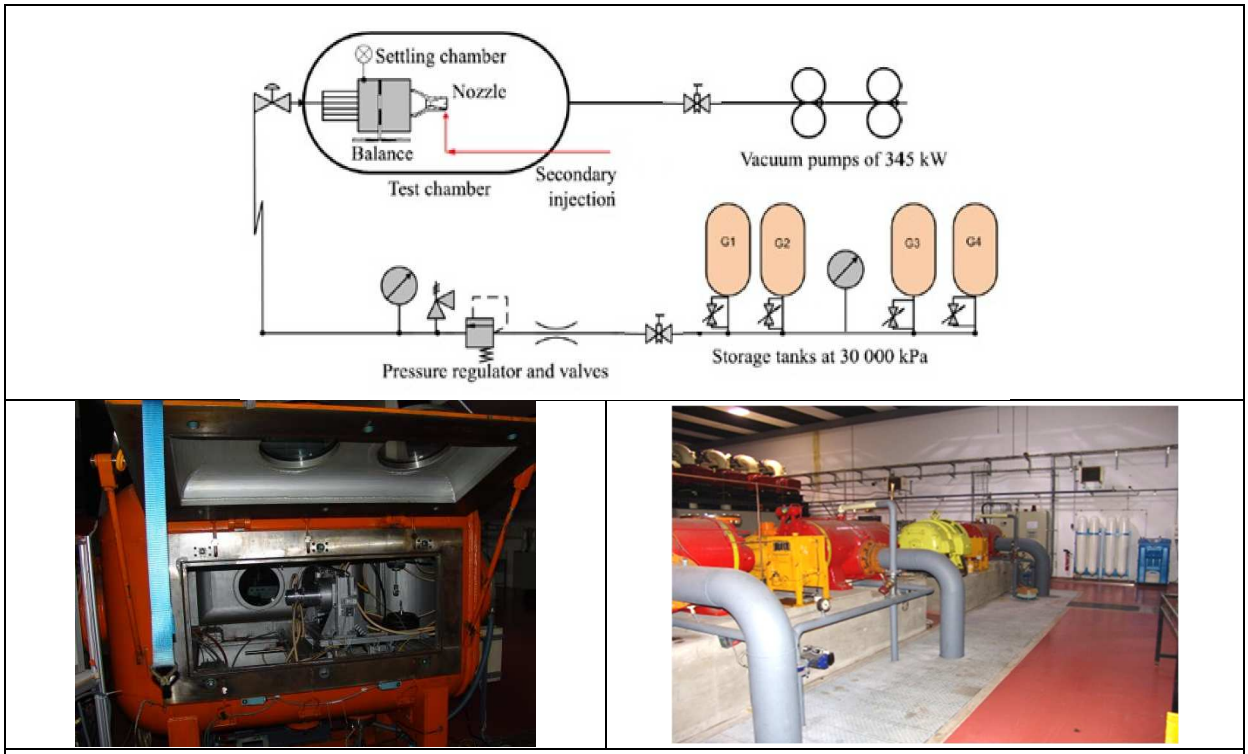

Figure 2 : The wind-tunnel EDITH test facility: Flow chart, test section photography (left), pumping group and storage tanks (right).

The force components exerted on the nozzle model were measured using a force balance system designed and constructed by the authors. The nozzle and its feeding chamber were mounted on the 3-frame force-balance system so that the assembly can move freely in the three orthogonal directions via frictionless bearings. Each frame is connected at one end of an HBM S2M S-shaped strain-gauge force transducer. The other ends of the transducers were fixed to the wind tunnel test section construction. The transducer signal was amplified to the 0-10 V range via an HBM RM4220 amplifier before being acquired by the National Instruments SCXI-1140 fast cards. Two symmetrically placed transducers of 200 N range were measuring the vertical (z-direction) force, one of 200 N range transducer was measuring the axial (Fx) force, while a smaller one of 20 N range transducer was installed to measure the (Fy) lateral force component. The force-balance with mounted test system was calibrated under static conditions using standard weights. From a large series of calibration measurement points, the transducer signal was treated and the standard deviations with maximum and relative error margins were evaluated. The balance was then qualified under static conditions and its reliability and repeatability were reported in [33]. In the current study, the standard deviation was found being in the range of 0.8%, while the absolute error was 3.5% for the measured side force. The dynamic calibration test was also carried out. It shows that the HBM resonance frequency is equal to 146Hz and that the sensor has a frequency pass-band range of 0.05 to 70 Hz.

Tests on the DBN flow regime transition were conducted imposing the constant inlet chamber pressure condition in one side and on the other side, by varying the test section ambient pressure. Roughly, it corresponds to reproducing 3 to 20 km of altitude, atmospheric flight conditions. In summary, employed diagnostics were composed of total pressure measurements in

the settling chamber and in the test section, 3-axes force balance and Z-Schlieren visualizations. The NI (National Instruments™) acquisition system was programmed to collect the raw pressure and force data with 1 kHz sample rate. Flow visualizations were obtained via Z-schlieren system and recorded using a 50 Hz frequency Canon®EOS60D camera.

Stagnation conditions	Nozzle geometry	Nozzle Flow conditions	Injection chamber: Geometry and injected flow conditions
P_t= 350 kPa T_0= 293 K ρ_0= 4.16 kg/m^3	**TIC Base nozzle:** - Length: L_b= 50.06 mm - Sonic throat radius: r_t= 8.5 mm - Exit diameter: d_{etic}= 32.16 mm **CP Extension Nozzle:** - Length: L_e= 36.72 mm - Exit diameter: d_e= 48,20 mm - Inflexion angle : α_i = 8° - Exit angle : α_e = 1.2°	- Mach number at inflection: M_{tic}=2.75 - Exit Mach number: M_e=3.16 - Pressure at inflection: 13717 Pa - Exit Pressure: 7418 Pa - Nozzle main mass flow rate: 187 g/s - Operating NPR range: from 10 to 100	- Injection slot width: 0.2 mm - Injection axial position: 8 mm from the inflection point -Injection direction: normal to the main axis - Settling chamber volume: 89.8 cm^3 - Settling chamber condition Pi: up to 77 kPa T_{inj} = 293 k

Table 1 : Main and secondary flow conditions and Nozzle geometric characteristics

The DBN nozzle design parameters (dimensions, mass flow rate…) were selected according to the operating capabilities of the facility. It corresponds to settling chamber pressure and temperature of 350 kPa and 290 K respectively, which, for a nozzle throat diameter of 17 mm leads to a theoretical mass flow rate of 0.187 kg/s. The nozzle contour was designed using the method of characteristics [34] [35] with an in-house built code. In this work, the first contour (from the throat to the inflection section) is based on a truncated ideal contour (TIC) for a theoretical exit Mach number of M_{tic}=2.75 and the second one is constructed assuming a constant wall pressure (Figure 3, right) for an exit Mach design M_e=3.16. Figure 3 (left) shows the test nozzle contour with secondary injection port and settling chamber geometries.

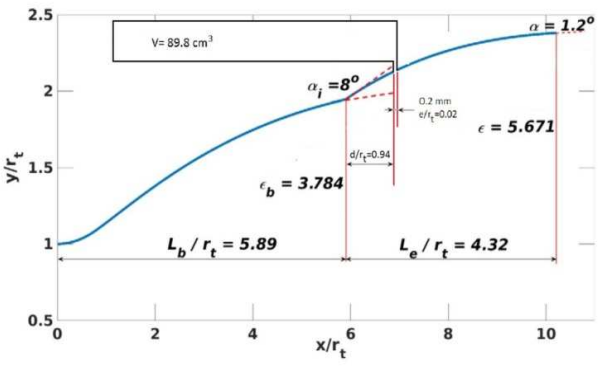

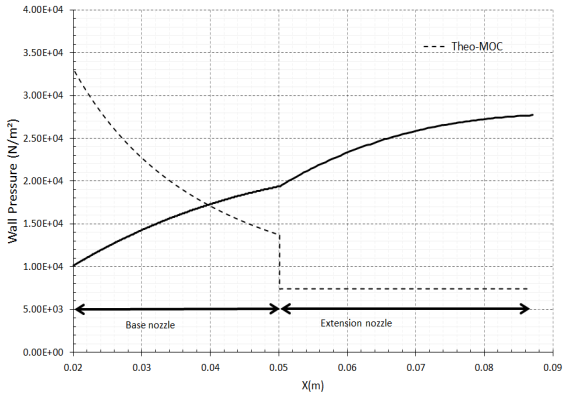

Figure 3 : Design of Dual-Bell Nozzle contour and secondary settling chamber (left), MOC wall pressure along the nozzle (right).

The nozzle was manufactured in two parts (Figure 4). This allowed creating a single continuous annular injection slot (between the two parts) placed 8 mm downstream the profile inflection with a width of 0.2 mm. This technique permits creating a settling chamber for the secondary injection aimed to obtain a homogeneous axisymmetric injection. The secondary injection direction was normal to the dual bell axis. The secondary settling chamber was fed by four 8 mm diameter tubes evenly distributed. The injection pressure was recorded by a large bandwidth micro (1.5 mm diameter) Kulite® XCQ-062 pressure transducer of 0-100 kPa range which was positioned in the settling chamber. The injection slot dimension and position were optimized and chosen based on previous similar work about shock-induced thrust vectoring carried out in the same facility [27-[29]. It is well known that with a secondary flow injection, the main flow responds with a bow shock. Consequently, an adverse pressure gradient and flow detachment occur upstream of the injection slot. In our experimental case, the secondary injection was placed sufficiently downstream of the inflection point of the profile in the goal to add this effect with the APG dominated flow region. Injecting in this manner allowed decreasing the slot width in the goal to decrease the secondary mass flow rate. All the operating conditions as well as the geometrical characteristics of the nozzles are presented in Table 1.

Figure 4 : Three dimensional Design of the DBN nozzle (left); two parts of the manufactured DBN nozzle (right).

2) Experimental results

One of the main originalities of the present experimental set-up is that it permitted the nozzle pressure ratio (NPR) variation by acting on the ambient pressure at the nozzle exit, while the nozzle feeding total pressure was kept constant. The ambient pressure variation is achieved by operating the main valve (partially opening or closing) located between the test chamber and the vacuum pumps (Figure 2).

Figure 5 shows, during a test, typical evolutions of the total pressure Pt, the ambient pressure at the test section Pa and the pressure at the secondary injection settling chamber Pi. The nozzle pressures ratio NPR (ratio of Pt to Pa) is also presented. We can observe that the total pressure (Pt) was well regulated and remained almost constant while the pressure in the test section (Pa) was

varied from 12 to 33 kPa. Consequently, the nozzle mass flow rate remained practically constant during the test case experimentation. Doing so, the NPR variation is only due to the test chamber pressure. This allowed a simple and direct force balance output recording versus the nozzle pressure ratio for a given nozzle mass flow rate. It's worth noting that, as long as the nozzle mass flow rate was kept constant, the variation of the force acting on the nozzle, recorded by the force balance device, was only a consequence of the variation of Pa. It should be noted, that this experiment was conducted without an effective fluid injection. The secondary settling chamber was closed upstream but remained open towards the nozzle primary flow. As the injection slot is located in the extension, logically as seen in Figure 5, the pressure in the cavity varied approximately between the ambient pressure (regime at sea level) and a pressure close to 7 kPa corresponding to an adapted flow in the extension (high altitudes regime). In other words, when the NPR increased, the secondary chamber was vacuumed and when the NPR decreased, the cavity was filled.

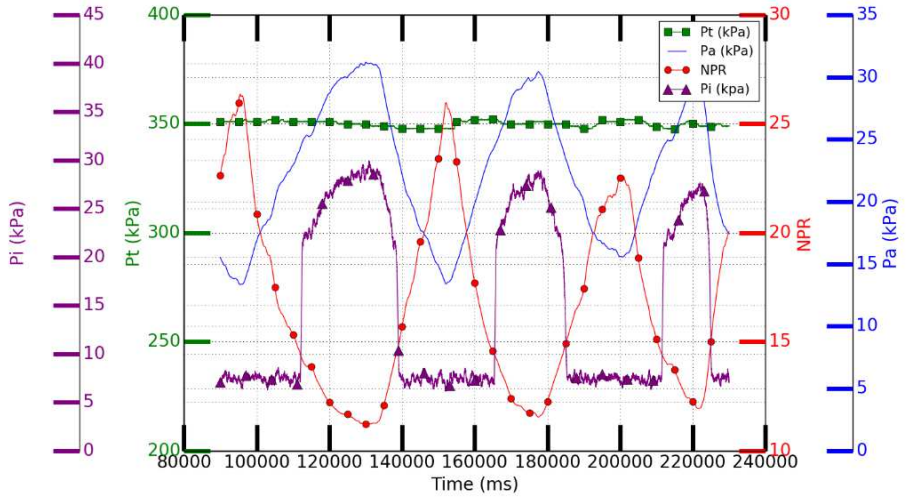

Figure 5 : Pressure and NPR evolutions versus time : Pa the ambient pressure (in the test section), Pt the total pressure (upstream of the dual bell), Pi the pressure inside the secondary stilling chamber, NPR the Nozzle Pressure Ratio (Pt/Pa)

Figure 6 shows side force component Fy (N), the specific impulse Isp (s), secondary pressures Pi and NPR variations versus time. In this case, the secondary injection was still not activated. As reported in [32], we can see that at each transition of regime, identified by the variation of the pressure in the secondary chamber, as expected the axial component of the force increased with increasing NPR. Additionally, at the expected transition, large peaks in the lateral force component (Fy) signal are clearly evidenced, while elsewhere, the average value of the signal is almost constant. Regarding the recorded axial thrust signal, reproducible “jumps” occurring at the same positions, corresponding to the flow transition and retransition respectively, are also observed. In our experimental conditions, it corresponds to a variation of about 4% of the nozzle thrust. This jump is downward when the NPR increases, and upward when it decreases. This is in accordance with the theoretical specific impulse curve depicted in Figure 1. Side loads are more intensive in the case of retransition (decreasing NPR, up to 4 N) compared to those observed at transition (increasing NPR, up to 1.5 N). This behavior is not reported in the literature. It can be noticed that lateral to axial forces ratio of about 1.5% is in the range of what is observed in the case of free shock separation in

conventional nozzles. It can be considered as an acceptable level for a DBN transition. Although the re-transition introduces unexpected higher side loads of about 5%, it still remains within the range reported for a restricted shock separation flow situation. We think this is due to the presence of the secondary feeding chamber. Indeed, this volume seems to have an action on the transition properties. By emptying it, it must produce an additional transient injection jet (blowing effect) to the main nozzle flow which seems to have an impact on the forces. A second hypothesis is that this volume isolates or dampens all or part of the pressure fluctuations coming from downstream. The observed effect can also be induced by the slot injection itself perturbing the boundary layer development or delaying the movement of the separation shock front. The retransition does not seem to be affected by the presence of the secondary injection settling chamber. In the following experiments, the NPR was kept constant and the change in flow regime is forced by means of the secondary injection.

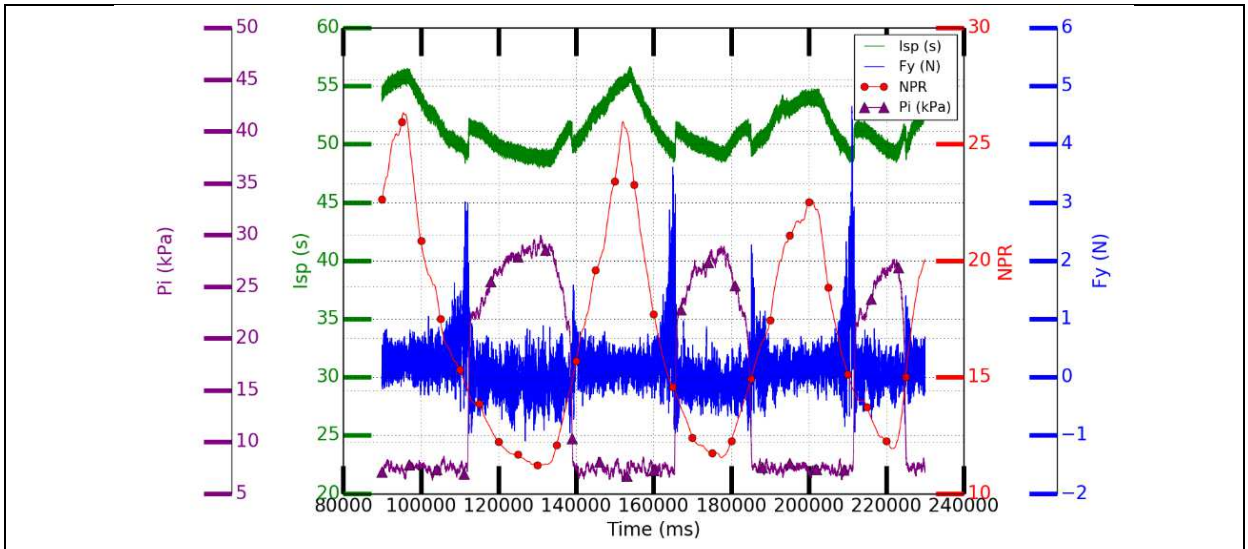

Figure 6 : ISP (s), lateral load (Fy, N), Secondary pressure (Pi) and NPR variation versus time, no pressure injection

a) Schlieren Visualisations

Figure 7 shows different wave configurations observed during the experiments at the nozzle exit and by extension inside the nozzle. In under expanded flow case (a), the figure depicts the inflection expansion fan (5) and the subsequent recompression shock (3). This shock is induced directly behind the wall inflection and it compresses the expanding core flow to the desired wall pressure [2]. The shock strength depends on the wall pressure profile prescribed within the nozzle design. As expected, the recompression shock reflects on the nozzle axis leading to the reflected shock (4). Downstream reflected shock interacts with expansion fan (2) issued from the nozzle lip. Finally, the jet boundary is also clearly visible (1). In over expanded flow case (b), in addition to the previous the case, as expected the reflection of the oblique shock wave (7) lead to a Mach disc (6). A reflected shock and a slip line (8) are issued from the triple point. The reflected shock is again reflected by the jet boundary (1). Also, the recompression shock (3) interacts with the oblique shock (7) of the same family forming, as expected, a single shock and a slip line is issued from the

intersection point. In the over expanded flow case (c) with secondary injection (11), a separation zone upstream of the injection slot is produced. The induced separation shock merge with the bow shock (9), formed by the fluidic obstacle, and coalescing into a single shock (10). This configuration has been described in previous work [27]. Downstream of fluidic obstacle, the flow is redirected toward the nozzle wall and creates a recompression shock (3).

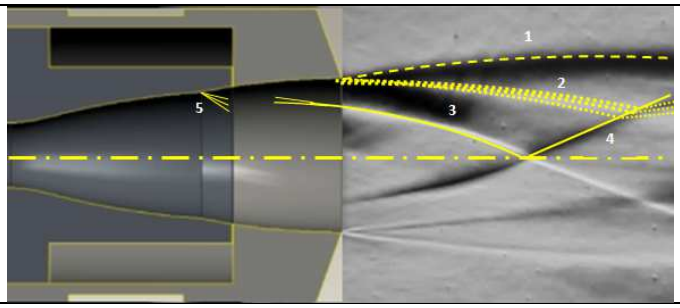

a) NPR=38.5, no injection, under expanded flow

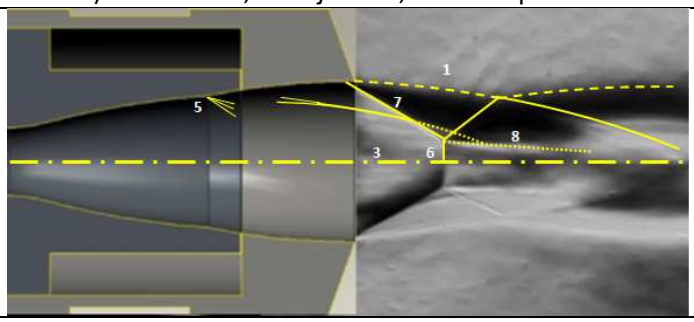

b) NPR=16.2, no injection, over expanded flow

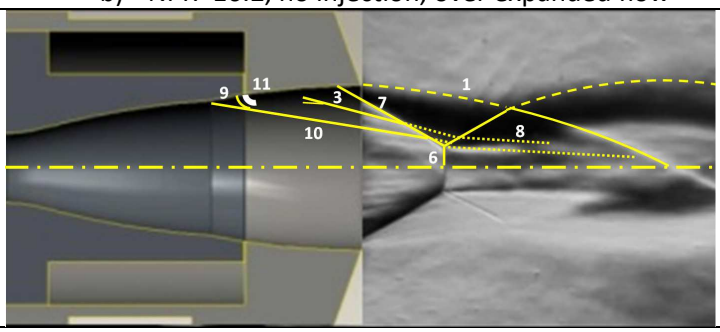

c) NPR=16.2, Pi=22.16 kPa, over expended flow with injection

1:jet boundary
2: nozzle lip expansion fan
3: recompression shock
4: reflected shock
5: inflection expansion fan
6: Mach disc
7: oblique shock
8: slip line
9: bow shock
10: separation shock
11: secondary injection jet

Figure 7 : Waves structure configurations for NPR =38.5 (a), NPR=16.2 (b) and NPR =16.2 with secondary injection (c). Dot line : slip line, dash line : jet boundary; line : shock wave

Figure 8 shows Schlieren visualizations of the forced transition and retransition by injection pressure variation. In this experiment, the NPR is kept constant close to 16. This value is slightly higher than the transition NPR, so that the flow regime configuration is in high altitude mode, i.e. with the flow attached to the base and to the extension nozzles. Then, first, the injection is activated by increasing the pressure in the secondary chamber and, thereafter, the flow is returned to its initial configuration by decreasing the injection pressure. It is observed in Figure 8 (a) that the increase in the secondary injection pressure induces the separation of the flow ahead of the injection slot and

subsequently favoring the detachment of flow in the whole extension section, thus forcing the retransition of the flow. The whole sequence of Schlieren visualization was recorded by a 50 Hz camera which had shown no instability (no flip-flopping) during the retransition. With this acquisition frequency, the images do not show the presence of high frequency instability. If there is flow instability, it occurs in maximum of 0.02 s duration time. The secondary injection induces a shock which allows the reduction of the Mach disc, typical of over expanded nozzle flows, then a retransition which is produced without upstream-downstream motion of the detachment point along the extension profile and with an axisymmetric flow behavior. It should be noted that flow regime transition is obtained for a low secondary injection pressure, around 33 kPa. When the injection pressure is reduced (Figure 8 (b)), the flow returns to its previous configuration characterized by an attached flow to the base and to the extension profiles. The transition takes place in an axisymmetric manner, without or with less observed instability which means a potentially lower side force. Flow transition also takes place when the secondary injection pressure drops below 33 kPa. It can be observed that this pressure value is close to that observed inside the settling chamber in low altitude mode flow regime (Figure 6). This confirms the hypothesis that the blowing effect due to the emptying of the cavity can explain the reduction of the observed lateral load at the transition.

a) Force measurement

For the experiment described in the previous section, Figure 9 shows the evolution of the nozzle specific impulse ISP, the pressure ratio NPR, the secondary injection pressure Pi and the lateral force component Fy as function of time. The specific impulse was calculated considering both the main and the secondary mass flow rates contributions. In this test-case of experiment, the nozzle pressure ratio was set constant (NPR ≈16). It can be observed that when the secondary pressure increases, the change of regime occurs and induces an ISP jump of about 2 seconds. The increase in ISP is due to the fact that the injection forces the flow to return to its optimal functioning regime (low altitude mode, Figure 1). Conversely, the overserved ISP decrease, when the injection pressure decreases, is due to the reattachment of the flow to the extension nozzle profile. The analysis of the measured lateral force component (Fy) shows that the strong peak intensity became undetectable during the forced transition and retransition. It confirms somehow the axisymmetric character of the flow as observed by the optical visualizations.

a) Retransition	b) Transition
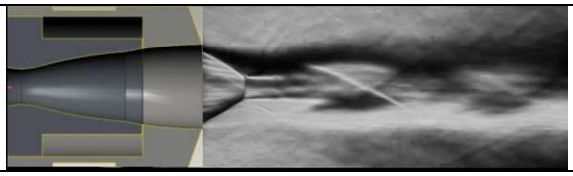	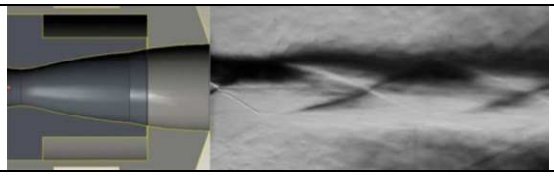
NPR=16.20, Pi=22.1 kPa, T=0 s	NPR=16.54, Pi=40.7 kPa, T=0 s
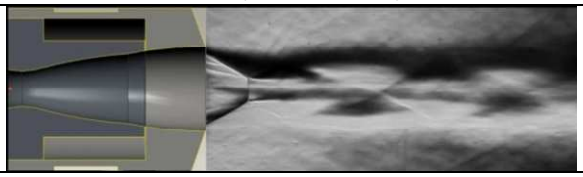	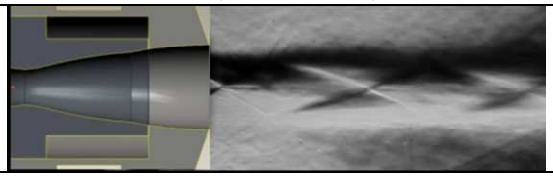
NPR=16.46, Pi=25.3 kPa, T=1.82 s	NPR=16.47, Pi=36.8 kPa, T=0.36 s
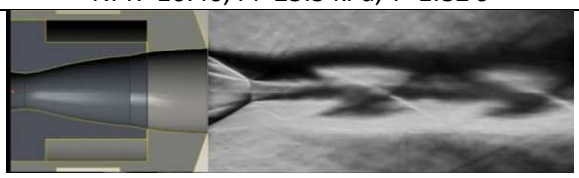	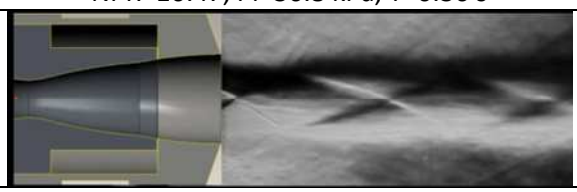
NPR=16.19, Pi=30.3 kPa, T= 3.54 s	NPR=16.53, Pi=33.2 kPa, T=0.78 s
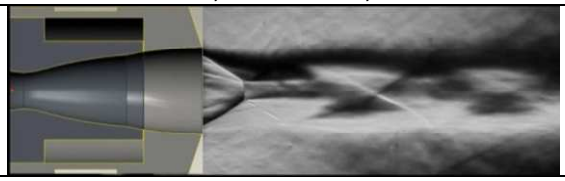	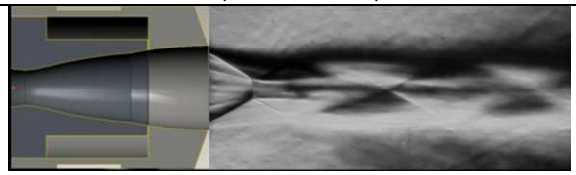
NPR=16.50, Pi=32.9 kPa, T= 4.52 s	NPR=16.53, Pi=33.0 kPa, T=0.80 s
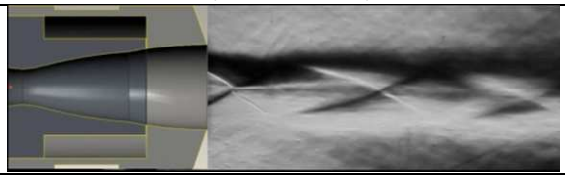	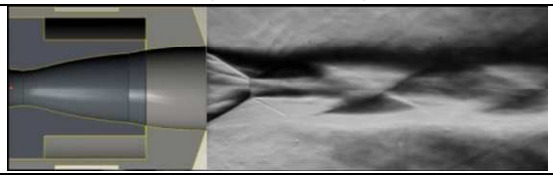
NPR=16.51, Pi=32.9 kPa, T=4.54 s	NPR=16.53, Pi=32.9 kPa, T=0.82 s
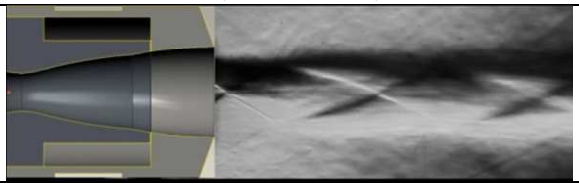	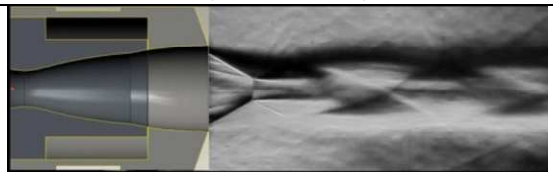
NPR=16.51, Pi=32.9, T=4.56 s	NPR=16.53, Pi=30.1, T=1.04 s
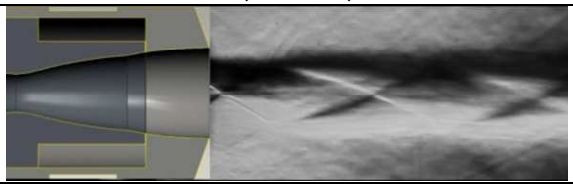	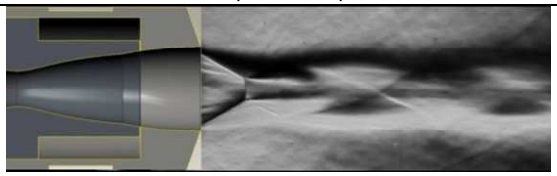
NPR=16.52, Pi=32.9, T=4.58 s	NPR=16.53, Pi=27.0, T=1.24 s

Figure 8 : Schlieren visualization of the forced transition and retransition by injection pressure variation. The NPR is kept constant

It should be noted, that the retransition is obtained for a secondary to main nozzles mass flow rates ratio of about 0.5% for a given NPR=16.5. For this NPR, the flow configuration is for the high-altitude mode. This NPR is close to the natural retransition (without injection) which is reached for NPR close to 14.8. The low value of secondary mass flow rate is obtained thanks to the position of the secondary injection downstream of the inflection point of the profiles.

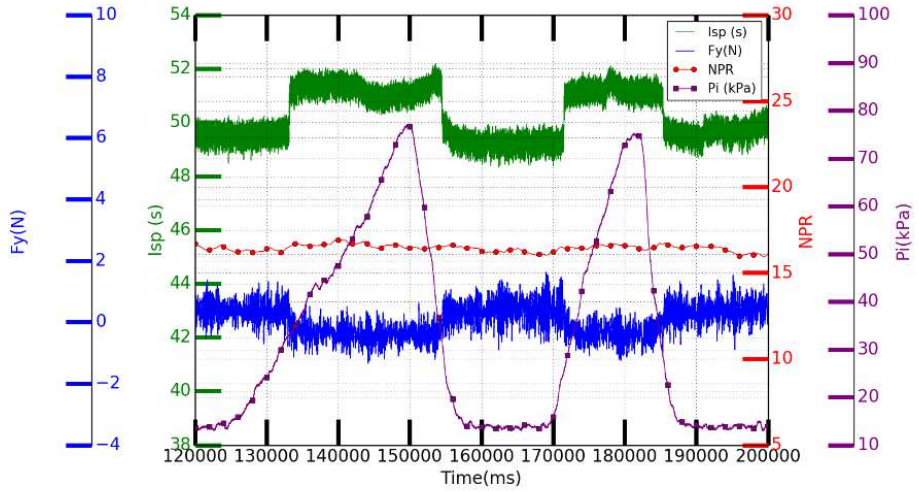

Figure 9 : Isp (s), axial load (Fy, N), Secondary pressure (Pi) and NPR variation versus time.

Figure 10 shows the evolution of the DBN specific impulse versus the secondary mass flow rate ratio *fm* during a sequence of increasing and then decreasing the secondary injection pressure. The transition and retransition occur at approximately 33 kPa for the injection pressure, i.e. for a ratio of the injected to the primary masse flow rates of approximately 0.52%. A small hysteresis during the transition-retransition cycle can, however, be observed.

As observed in the previous works on fluidic trust vectorization [29], the secondary injection into the supersonic nozzle flow induces a wall pressure increase upstream of the injection port due to the separation shock induced by the fluidic obstacle. This effect is then coupled with the adverse pressure gradient (APG) dominated inflection region and enhances the flow detachment from the extension nozzle by mean of such low secondary mass flow rate. The effect of the secondary injection is therefore to avoid the attachment of the flow at the extension wall. This coupling effect is made possible by injecting downstream of the inflexion region (8 mm in our case). Compared to the works of Tomita et al. [25] and Ferro et al. [26] where the radial injection was placed at the inflection point, the downstream secondary injection port position may have a strong influence on the flow regime transition with low secondary mass flow rate (2% compared to 4 - 7.7%). We think that the wall pressure in the area between the injection port and the profile inflection is an important parameter controlling the detachment. It was confirmed by Takahashi et al. [36] in hot-flow testing of dual-bell nozzle experiment. It indicates that the separation transition condition is strongly related to the wall pressure in the inflection region. The secondary injection also induces an additional shock wave which increases the flow pressure inside the extension nozzle. The difference between the jet

pressure and the ambient pressure is therefore reduced and high over expanded flow regime configurations are avoided or limited.

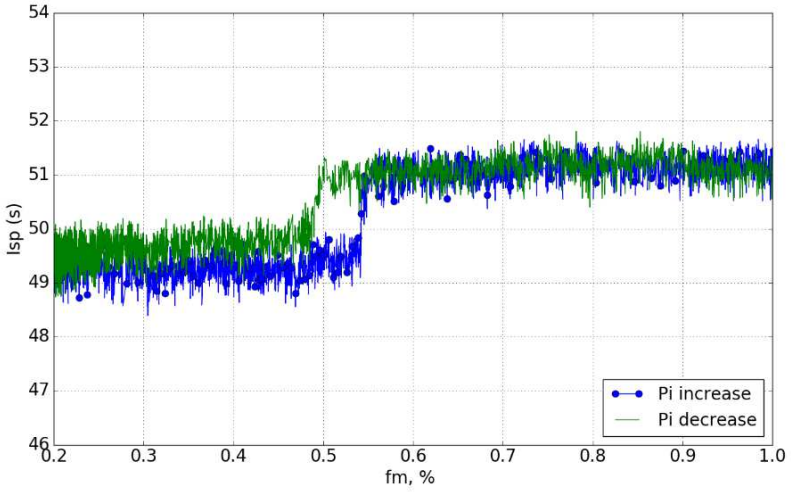

Figure 10 : Evolution of the specific impulse Isp versus the secondary mass flow rate ratio fm during a sequence of increasing and then decreasing the secondary injection pressure

3) Summary and conclusion

The current study further investigates and analyses the proposed method of active flow regime transition control in a dual-bell rocket nozzle reported previously in [31, 32]. The main focus of the present work was the influence of secondary injection characteristics on the flow transition in DBN. In the studied nozzle model, the first profile is an ideal contour and the second one is constructed hypothesizing a constant pressure profile. The nozzle is manufactured in two parts. This allows creating a single continuous annular injection slot placed on 8 mm downstream the profile inflection with a width size of 0.2 mm and a secondary settling chamber. Pressure measurement, Schlieren visualization and thrust and side loads have been reached.

Without secondary injection, experimental results show lower lateral load peak during the transition (when the NPR increases) compared to the retransition case (when the NPR decreases). The secondary settling chamber volume seems to have an action on the properties of the transition. It must produce a small injection jet (blowing effect) which may have an impact on transition phenomenology and consequently on lateral load. A second hypothesis is that this volume isolates or dampens all or part of the pressure fluctuations coming from downstream.

We show that that a secondary fluidic injection placed downstream of the inflection region can force the flow to retransition, from high altitude regime to sea level altitude regime. This forced retransition was reached without measurable side loads, for low secondary injection mass flow rate (0.5%) and was characterized by an ISP jump. When the injection pressure is reduced, the flow returns to its natural configuration (high altitude flow regime). The transition from the low altitude forced regime to the high-altitude regime is then observed. This transition is characterized by an ISP fall and is also achieved without measurable side loads. This flow control technique allows

overcoming the main problem preventing the use of these nozzles and can be implemented for transition and retransition control that could be interesting in reusable satellite launchers development context. These initial results are very encouraging and the technique has been the subject of a patent application. In an increasingly competitive sector, the performance increase made by the possible use of dual bell nozzles could reduce the access cost to space.

ACKNOWLEDGELENTS

We would like to gratefully acknowledge the laboratory of Excellence CAPRYSSES framework and the financial support of this study from grant No. ANR-11-LABX-0006-01 of the “Investissements d'Avenir LabEx CAPRYSSES”. We would also like to thank Nicolas Gouillon of ICARE/CNRS and Michael Burman of LMEE/Univ-Evry-Paris-Saclay for their technical assistance and Matthieu Sammut of CNRS for his assistance during patent filing.

References

[1] M. Frey, G. Hagemann, Critical assessment of dual-bell nozzles, J. Propuls. Power 15(1) (1999) 137-143, https://doi.org/10.2514/2.5402.

[2] G. Hagemann, M. Terhardt, D. Haeseler, Experimental and analytical design verification of the dual-bell concept, J. Propuls. Power 18(1) (2002) 116-122, https://doi.org/10.2514/2.5905

[3] G. Hagemann, H. Immich, T.V. Nguyen, G.E. Dumnov, Advanced rocket nozzles, J. Propuls. Power 14(5) (1998) 620-634, https://doi.org/10.2514/2.5354.

[4] R. Stark, C. Genin, D. Schneider, C. Fromm, Ariane 5 performance optimization using dual-bell nozzle extension, J. Spacecr. Rockets 53(4) (2016) 743–750, https://doi.org/10.2514/1.A33363.

[5] W.C. Swan, The Influence of Nozzle Design on the Flight Performance of Rocket Vehicles, with an Analysis of the Results of Jet Separation, Master’s thesis, California Institut of Technology, Pasadena, CA, United States, (1948), http://thesis.library.caltech.edu/239/.

[6] C.R. Foster, F.B. Cowles, Experimental Study of Gas-Flow Separation in Overexpanded Exhaust Nozzles for Rocket Motors, Tech. Rep. JPL-PR-4-103, Jet Propulsion Laboratory, California Institut of Technology, Pasadena, CA, United States, (1949), http://hdl.handle.net/2060/19630039654.

[7] A.T. Sutor, Rockwell International Corp. assignee, Step nozzle, US patent 339,454,9 A, (1968), http://pdfpiw.uspto.gov/.piw?Docid=03394549.

[8] C. Nurnberger-Genin, R. Stark, Flow transition in dual bell nozzles, Shock Waves 19(3) (2009) 265–270, https://doi.org/10.1007/s00193-008-0176-4.

[9] C. Genin, R.H. Stark, Side loads in subscale dual bell nozzles, J. Propuls. Power 27(4) (2011) 828–837, https://doi.org/10.2514/1.B34170.

[10] C. Nurnberger-Genin, R. Stark (2010), Experimental Study on Flow Transition in Dual Bell Nozzles, Journal of Propulsion and Power, 26, pp 497-502.

[11] Génin, C., Gernoth, A., Stark, R. (2013), “Experimental and Numerical Study of Heat Flux in Dual Bell Nozzles,” Journal of Propulsion and Power, Vol. 29, No. 1, , pp. 21–26. https://doi.org/10.2514/1.B34479

[12] Verma S.B., Stark R., Haidn O. (2012), Gas density effects on dual-bell transition behavior, J. Propuls. Power 28(6) 1315–1323, https://doi.org/10.2514/1.B34451.

[13] Verma S.B., Stark R., Haidn O. (2013), Reynolds number influence on dual-bell transition phenomena, J. Propuls. Power 29(3) 602–609, https://doi.org/10.2514/1.B34734.

[14] Verma S.B., Stark R., Haidn O. (2014), Effect of ambient pressure fluctuations on dual-bell transition behavior, J. Propuls. Power 30(5) 1192–1198, https://doi.org/10.2514/1.B35067

[15] Verma S.B., Hadjadj A., Haidn O. (2015), Unsteady flow conditions during dual-bell sneak transition, J. Propuls. Power 31(4) 1175–1183, https://doi.org/10.2514/1.B35558.

[16] Reijasse, P., Coponet, D., Luyssen, J.-M., Bar,V., Palerm, J., Oswald, J.,Amouroux, F., Robinet, J.-C., and Kuszla, P. (2011), Wall Pressure and Thrust of a Dual Bell Nozzle in a Cold Gas Facility, Progress in Propulsion Physics, Vol. 2, pp. 655–674. https://doi.org/10.1051/eucass/201102655

[17] Martelli E., Betti B., Nasuti F. (2014), Flow separation response to unsteady external disturbances in dual bell nozzles, in: Proceedings of the 50th Joint Propulsion Conference & Exhibit, no. 2014-3998, AIAA, Cleveland, OH, United States, pp.1–11.

[18] Nasuti F., Martelli E., Onofri M. (2005), Role of wall shape on the transition in axisymmetric dual-bell nozzles, J. Propuls. Power 21(2) 243–250, https://doi.org/10.2514/1.6524.

[19] Kimura T., Niu K., Yonezawa K., Tsujimoto Y., Ishizaka K. (2009), Experimental and analytical study for design of dual-bell nozzles, in: Proceedings of the 45th Joint Propulsion Conference & Exhibit, no. 2009-5149, AIAA, Denver, CO, United States, pp.1–9.

[20] Proshchanka D., Yonezawa K., Koga H., Tsujimoto Y., Kimura T., Yokota K. (2012), Jet oscillation at low-altitude operation mode in dual-bell nozzle, J. Propuls. Power 28(5) 1071–1080, https://doi.org/10.2514/1.B34466.

[21] R. Stark, C. Genin, Sea-level transitioning dual bell nozzles, CEAS Space J., doi 10.1007/s12567-017-0154-8

[22] E. Martelli, F. Nasuti, M. Onofri, Numerical analysis of film cooling in advanced rocket nozzles, AIAA J. 47(11) (2009) 2558–2565, https://doi.org/10.2514/1.39217.

[23] R. Stark, C. Genin, Hot flow testing of a film cooled dual bell nozzle, in: Proceedings of the 47th Joint Propulsion Conference & Exhibit, no. 2011-5614, AIAA, San Diego, CA, United States, 2011, pp.1–9

[24] D. Proshchanka, K. Yonezawa, H. Koga, Y. Tsujimoto, T. Kimura, K. Yokota, Control of operation mode transition in dual-bell nozzles with film cooling, J.Propuls. Power 28(3) (2012) 517–529, https://doi.org/10.2514/1.B34202.

[25] Tomita, M. Takahashi, M. Sasaki, Control of transition between two work-ing modes of a dual-bell nozzle by gas injection, in: Proceedings of the 45th Joint Propulsion Conference & Exhibit, no. 2009-4952, AIAA, Denver, CO, United States, 2009, pp.1–6.

[26] A. Ferro, E. Martelli, F. Nasuti, D. Pastrone, " Fluidic control of transition in a dual bell nozzle", AIAA propulsion and energy forum 2020, virtual event, doi 10.2514/6.202063788

[27] V. Zmijanovic, L. Leger, E. Depussay, M. Sellam, A. Chpoun, Experimental–numerical parametric investigation of a rocket nozzle secondary injection thrust vectoring, J. Propuls. Power 32(1) (2016) 196–213,

[28] V. Zmijanovic, V. Lago, M. Sellam, A. Chpoun, Thrust shock vector control of an axisymmetric conical supersonic nozzle via secondary transverse gas injection, Shock Waves 24(1) (2016) 97–111, https://doi.org/10.1007/s00193-013-0479-y.

[29] V. Zmijanovic, V. Lago, L. Léger, E. Depussay, M. Sellam, A. Chpoun, "Thrust vectoring effects of a transverse gas injection into a supersonic cross-flow of an axisymmetric C-D nozzle", Advances in Aerospace Sciences book, Vol.4, Progress in Propulsion physics edition, pp. 77-106, 2013

[30] V. Zmijanovic, L. Léger, M. Sellam, A. Chpoun, "Assessment of transition regimes in dual bell nozzle and possibility of active fluidic control", Aerospace Science and Technology, doi: 10.1016/j.ast.2018.02.003, Vol. 82–83, pp. 1-8, November 2018.

[31] L. Léger, V. Zmijanovic, M. Sellam, A. Chpoun, "Contrôle de transition de régime et de vectorisation de poussée dans une tuyère à galbe multiple par injection secondaire", déposé le 18/04/2018, FR3080407, PCT 25/10/19. https://bases-brevets.inpi.fr/fr/document/FR3080407.html?s=1572864632551&p=6&cHash=92756e10cbc8491a51123c249d157dea

[32] L. Léger, V. Zmijanovic, M. Sellam, A. Chpoun, "Controlled Flow Regime Transition in a Dual Bell Nozzle by Secondary Radial Injection", Experiments in Fluids (2020) 61:246, doi: 10.1007/s00348-020-03086-3

[33] V. Zmijanovic, "Vectorisation fluidique de la poussée d'une tuyère axisymétrique supersonique par injection secondaire", PhD thesis, Orléans University, 2013.

[34] M.J. Zucrow, J.D. Hoffman, Gas Dynamics, vol. 1, John Wiley and Sons, Inc., New York, United States, 1976.

[35] M.J. Zucrow, J.D. Hoffman, Gas Dynamics – Multidimensional Flow, vol. 2, John Wiley and Sons, Inc., New York, United States, 1977.

[36] H. Takahashi, T. Tomita, C. Genin, D. Schneider, "LOX/CH4 Hot-Flow Testing of Dual-Bell Nozzles with Rapid-Expansion Extension", J. of Prop. And Power, 34(5), 1214-1224, 2018, doi: 10.2514/1.B36768